HHS Public Access

Author manuscript

Nat Immunol. Author manuscript; available in PMC 2016 May 01.

Published in final edited form as:

Nat Immunol. 2015 November ; 16(11): 1124–1133. doi:10.1038/ni.3272.

Runx3 specifies lineage commitment of innate lymphoid cells

Takashi Ebihara[1], **Christina Song**[2], **Stacy H. Ryu**[2], **Beatrice Plougastel-Douglas**[3], **Liping Yang**[3], **Ditsa Levanon**[4], **Yoram Groner**[4], **Michael D. Bern**[3,5], **Thaddeus S. Stappenbeck**[2], **Marco Colonna**[2], **Takeshi Egawa**[2], and **Wayne M. Yokoyama**[1,3]

[1]Howard Hughes Medical Institute, Washington University School of Medicine, St. Louis, MO 63110 USA

[2]Department of Pathology and Immunology, Washington University School of Medicine, St. Louis, MO 63110 USA

[3]Division of Rheumatology, Department of Medicine, Washington University School of Medicine, St. Louis, MO 63110 USA

[4]Department of Molecular Genetics, The Weizmann Institute of Science, Rehovot, Israel

[5]Medical Scientist Training Program, Washington University School of Medicine, St. Louis, MO 63110 USA

Abstract

Subsets of innate lymphoid cells (ILCs) reside in the mucosa and regulate immune responses against external pathogens. While ILCs can be phenotypically classified into ILC1, ILC2 and ILC3 cells, the transcriptional control of lineage commitment for each ILC subset is incompletely understood. Here we report that the transcription factor Runx3 was essential for normal development of ILC1 and ILC3, but not ILC2 cells. Runx3 controlled the survival of ILC1, but not ILC3 cells. Runx3 was required for the expression of RORγt and its downstream target, aryl hydrocarbon receptor, in ILC3 cells. The absence of Runx3 in ILCs exacerbated *C. rodentium* infections. Therefore, our data establish Runx3 as a key transcription factor for lineage-specific differentiation of ILC1 and ILC3 cells.

Innate lymphoid cells (ILCs) reside in mucosal surface to facilitate immune responses, maintain mucosal integrity, and promote lymphoid organogenesis[1]. They do not express rearranged antigen-specific receptors, are dependent on IL-2Rγc for differentiation, and all ILCs in the intestine express IL-7Rα (CD127), which forms a heterodimer with IL-2Rγc. The ILC populations are classified into three groups, ILC1, ILC2 and ILC3, based on the expression of specific cytokines, similar to T cell subsets[1]. ILC1 cells are characterized by their capacity to produce the type 1 cytokine interferon γ (IFN-γ) in response to interleukin

Correspondence should be addressed to W. M. Y. (yokoyama@dom.wustl.edu).

AUTHOR CONTRIBUTION

T.Eb. and W.M.Y. designed experiments and analyzed data; T.Eb., L.Y., C.S., S.H.R., B.P.-D., T.S.S. and M.D.B. performed the experiments; D.L. and Y.G. supplied critical reagents; T.Eg. analyzed ChIP sequence data; T.Eb., T.Eg., Y.G., M.C., T.S.S. and W.M.Y. wrote the paper.

12 (IL-12), IL-15 and IL-18. ILC2 cells respond to IL-25 and IL-33 and secrete a set of T_H2 cytokines IL-5, IL-9, IL-13 and amphiregulin. ILC3 cells share many features with T_H17 and T_H22 cells and can be stimulated by IL-1 and IL-23 to elicit IL-17 and IL-22 production. ILC3 cells are heterogeneous and can be further subdivided into additional subsets by expression of CD4 and NKp46: $CD4^+$ ILC3, $NKp46^+$ ILC3 (also known as NK22 or ILC22) and double negative (DN) ILC3 cells[1]. Fetal ILC3 cells in intestine are $CD4^-$ or $CD4^+$ lymphoid tissue inducer (LTi) cells, which are necessary for the development of lymph nodes and Peyer's patches (PPs)[2]. $NKp46^+$ ILC3 cells specifically produce only IL-22, but not IL-17[1,3,4] and have the potential to differentiate into IFN-γ-producing ILC1 cells[4,5]. Thus, ILCs can be classified into different subsets which can be distinguished and they play distinct roles in immune responses.

With regard to their differentiation and transcriptional regulation, all ILC lineages are derived from common lymphoid progenitor cells (CLPs), which also give rise to B cells and T cells[1]. The earliest progenitor cells specific to ILCs are $CXCR6^+$ integrin α4β7-expressing CLPs ($CXCR6^+$ αLP), which have the potential to differentiate into ILC1, ILC2, ILC3, and splenic NK cells[6]. The transcription factor NFIL3 (E4BP4) is essential for differentiation of $CXCR6^+$ αLPs and all ILC lineages. The common progenitors to all helper-like innate lymphoid cell lineages (CHILP) are defined by the Lin^- $CD127^+$ $Id2^+$ $CD25^-$ $\alpha4\beta7^+$ phenotype and give rise to ILC1, ILC2 and ILC3 cells, but not splenic NK cells[5]. In this context, NK cells could be a different subset, distinct from ILC1 cells. The common precursor to ILC (ILCP) is identified by the expression of the transcription factor PLZF and can generate ILC1, ILC2 and ILC3 cells although they do not differentiate into the $CD4^+$ ILC3 subset and splenic NK cells[7]. PLZF is expressed in a proportion of CHILPs, suggesting that they are precursors of ILCPs[5]. However, the ILC lineage specification process downstream of ILCPs remains to be completely elucidated.

Differentiation of each ILC subset requires specific transcription factors[1]. While ILC1 cells in the intestine are $DX5^-$ and do not express the transcription factor Eomes, splenic NK cells are $DX5^+$ $Eomes^+$ and appear to be dependent on Eomes for full maturation[1,5]. Although both ILC1 cells and splenic NK cells express T-bet, a T_H1 transcription factor, ILC1 cells in the intestine are highly dependent on T-bet, whereas splenic NK cells are only modestly affected by the absence of T-bet[1,5,8]. ILC2 cells require GATA-3, a T_H2 transcription factor, and RORα for their development[9–11]. The transcription factor RORγt is required for ILC3 and deficiency of aryl hydrocarbon receptor (AHR) affects all ILC3 subsets[1,12,13], suggesting a potential link between RORγt and AHR in ILC3 cells that has not been elucidated. Both RORγt and AHR transcription factors are also indispensable to T_H17 and T_H22 cells[14]. Of the ILC3 subsets, only $NKp46^+$ ILC3 cells express and require T-bet. Although earlier studies suggested that GATA-3 is an ILC2-specific transcription factor[1,10], recent studies argue that an intermediate level of GATA-3 is also expressed in ILC1 and ILC3 cells and regulates these populations through maintaining CD127 expression[5,9,15]. Thus, the requirements of transcription factors studied thus far for specification of ILC subsets are generally similar to those in helper T cells.

The Runx family of transcription factors, especially Runx1 and Runx3, play important roles in the development of various hematopoietic lineages, including T cells[16]. Runx1 is essential

for the emergence of hematopoietic stem cells from hemogenic endothelial cells and the development of lymphoid and dendritic cell progenitors, megakaryocytes, Foxp3$^+$ regulatory T cells and T_H17 cells[16,17]. Runx3 is important for differentiation of CD8$^+$ T cells, T_H1 and splenic NK cells[16,18]. The majority of phenotypes resulting from deficiency of Runx1 or Runx3 are more pronounced with deletion of *Cbfb*, encoding the common obligatory partner (CBF-β) of all Runx proteins, suggesting that Runx family members play overlapping roles in immune cell development and function[16].

An early study, before the identification of ILC progenitor cells, described a reduction in the numbers of PPs and RORγt$^+$ LTi cells in the fetal intestine in mice lacking the main transcript variant of Runx1 or CBF-β[19]. Deficiency of Runx1 or CBF-β in hematopoietic cells affects Flt3$^+$ progenitor cells including CLPs[17], suggesting that reduced numbers of fetal intestine RORγt$^+$ LTi cells in the absence of Runx1 or CBF-β[19] could be due to effects on CLPs, the precursors to all ILCs. Therefore, the requirements for Runx proteins in the differentiation of ILCs have not been clearly defined.

Here we show that among the three Runx family members, *Runx3* derived from its distal promoter was specifically expressed in ILC1 and ILC3 cells, but not ILC2 cells. Specific deletion of *Cbfb* or *Runx3* using NKp46-Cre resulted in marked reduction of ILC1 and NKp46$^+$ ILC3 cells in the intestine, which led to poor control of *C. rodentium* infection. *Runx3* deletion in hematopoietic cells did not affect the numbers of CLP, αLP, CHILP and ILCP, but abrogated RORγt expression and subsequent AHR expression by all ILC3 subsets in intestine. Thus, our data reveal the non-redundant role of Runx3 in differentiation of ILC1 and ILC3 cells.

RESULTS

Distal Runx3 is expressed in ILC1 and ILC3, not ILC2

We first examined the expression of *Runx1, Runx2, Runx3* and *Cbfb* in ILC1 cells from murine small intestinal epithelium, ILC2 cells and all ILC3 subsets from murine small intestinal lamina propria. Among Runx family members, *Runx3* transcripts were predominantly expressed in all ILCs (Fig. 1a). All Runx family members including Runx3 can be expressed in two forms which originate from a proximal or distal promoter[20], with distal *Runx3* transcripts being dominant in lymphocytes[20–22]. Although proximal *Runx3* transcripts are poorly translated into protein in CD4$^+$ T cells which express only proximal *Runx3*, CD8$^+$ T cells use the distal *Runx3* promoter for Runx3 protein expression[21,22]. To discriminate between proximal and distal promoter usage in ILCs, we further examined *Runx3* expression in ILCs by RT-PCR and in *Runx3d*$^{+/YFP}$ mice expressing a membrane bound YFP from the distal *Runx3* promoter[22]. Whereas ILC1 and ILC3 cells expressed only distal *Runx3*, expression of *Runx3* in ILC2 cells was driven only by the proximal promoter (Fig. 1b,c). Splenic NK cells expressed both *Runx3* transcripts but less distal *Runx3*, as previously observed[18]. The expression of distal Runx3 was highest in ILC1 cells, moderate in ILC3 cells, low in splenic NK cells and undetectable in ILC2 cells (Fig. 1b,c). NK cells in liver and skin are known to segregate into two subsets, DX5$^-$ CD49a$^+$ tissue-resident NK (trNK) cells and DX5$^+$ CD49a$^-$ conventional NK cells[23]. The trNK cells in the liver expressed more distal Runx3 than DX5$^+$ CD49a$^-$ conventional NK cells (Supplementary

Fig. 1a). By contrast, distal Runx3 expression by both NK populations in the skin was low. While CD49a and DX5 expression on salivary gland NK cells was not previously described and their tissue-residency has not been determined, their distal Runx3 expression was very high (Supplementary Fig. 1a). Thus, distal Runx3 is preferentially expressed in the ILC1 and ILC3 subsets, but not ILC2 cells.

We next examined ILC progenitors in adult bone marrow for distal *Runx3* and other Runx expression by RT-PCR and reporter expression in *Runx3d*$^{+/YFP}$ mice. While expression of all Runx family members was relatively low in CLPs, αLPs and CHILPs from adult bone marrow, ILCPs strongly expressed *Runx1* and *Runx3* transcripts (Fig. 1d). Distal Runx3 expression in ILCPs was also confirmed in ILCPs isolated from *Runx3d*$^{+/YFP}$ mice (Fig. 1e). A small fraction of CHILPs in bone marrow of *Runx3d*$^{+/YFP}$ mice was PLZF^{+}, and these cells expressed YFP driven from distal *Runx3* promoter (Fig. 1e,f), suggesting PLZF^{+} ILC progenitor cells start expressing distal Runx3 before ILC lineage specification. Because ILC2 cells and ILC2 precursors (ILC2Ps) did not have substantial distal Runx3 expression based on absent YFP expression in these cells in *Runx3d*$^{+/YFP}$ mice (Fig. 1c,e), the apparent loss of distal Runx3 expression seems to be an ILC2-specific event. However, ILC1 cells maintain high level of distal Runx3 expression, and ILC3 cells down-regulate distal Runx3 but still maintain a moderate level of distal Runx3 expression. These data suggest that Runx3 may contribute to ILC lineage specification.

CBF-β is indispensable to NKp46^{+} ILC3 and ILC1 in intestine

Because Runx family members can bind to the same Runx-binding motif, other Runx proteins could potentially compensate for the deficiency of another Runx family member[16,21]. To examine the roles of Runx family members in ILC1 and ILC3 cells, we sought to delete the function of Runx3 and other Runx family members by deleting their binding partner CBF-β. We generated mice with an intrinsic *Cbfb* deletion in NKp46-expressing cells, ILC1 and NKp46^{+} ILC3 cells, by crossing *Cbfb*$^{f/f}$ mice with NKp46-Cre mice. *Cbfb*$^{f/f}$ NKp46-Cre mice lacked NKp46^{+} ILC3 cells in the small intestine, colon and PPs (Fig. 2a,b and Supplementary Fig. 1b,c). In addition, the numbers of other NKp46-expressing cells including ILC1 cells in intestine and NK cells in spleen, liver, salivary gland and skin were also strongly reduced in *Cbfb*$^{f/f}$ NKp46-Cre mice (Fig. 2c,d and Supplementary Fig. 1d,e). By contrast, differentiation of other ILC3 subsets were not affected by CBF-β deficiency (Fig. 2a,b). Thus, CBF-β expression in NKp46^{+} cells appears to be required for the development of ILC1 and NKp46^{+} ILC3 lineages.

To address the possibility that NKp46^{+} ILC3 cells lacking CBF-β were not able to express NKp46, we examined NKp46 expression in splenic NK cells and found that it was not changed by CBF-β deficiency (Supplementary Fig. 1d). Blimp-1 is preferentially expressed in NKp46^{+} ILC3 cells but not in other ILC3 subsets, and is not necessary for the differentiation of NKp46^{+} ILC3 cells[24]. This finding was recapitulated here (Fig. 2e), allowing us to examine the expression of *Blimp-1* transcripts in *Cbfb*$^{f/f}$ and *Cbfb*$^{f/f}$ NKp46-Cre ILC3 (RORγt-GFP^{+}) cells in *Rorc*(gt)$^{wt/gfp}$ mice to test the possibility that CBF-β deficiency abrogated NKp46 expression, but NKp46^{+} ILC3 cells were otherwise unaffected. *Blimp-1* expression was comparably low in *Cbfb*$^{f/f}$ and *Cbfb*$^{f/f}$ NKp46-Cre NKp46^{-} ILC3

(RORγt-GFP$^+$) cells (Fig. 2e), suggesting CBF-β deficiency does not affect only NKp46 expression in ILC3 cells in *Cbfb*$^{f/f}$ NKp46-Cre mice. These results suggest that CBF-β is required for the development of NKp46$^+$ ILC3 cells, suggesting that Runx family members may be required for ILC subset differentiation.

Runx3 is required for ILC1 and intestinal ILC3 development

To analyze the effect of Runx3-deficiency in all hematopoietic cells including ILCPs and all ILC3 subsets, we studied *Runx3*$^{f/f}$ Vav1-Cre mice in which *Runx3* is deleted in hematopoietic cells. We found a comparable number of CLPs, αLPs, CHILP, ILC2P and ILCPs in the bone marrow of *Runx3*$^{f/f}$ Vav1-Cre mice compared to *Runx3*$^{+/f}$ Vav1-cre control mice (Supplementary Fig. 2). Because ILCPs expressed comparable amounts of Runx1 and Runx3 (Fig. 1d), Runx1 might compensate for the loss of Runx3 in these cells. The number of Peyer's patches (PPs) was reduced in *Runx3*$^{f/f}$ Vav1-Cre mice compared to *Runx3*$^{+/f}$ Vav1-cre control mice (Fig. 3a). No RORγt$^+$ ILC3 subsets were detectable in the remaining PPs and lamina propria lymphocytes (LPLs) in *Runx3*$^{f/f}$ Vav1-Cre mice (Fig. 3b,c). These data suggest a defect in ILC3 cell development in the setting of Runx3-deficiency.

We then examined if Runx3 deletion in NKp46-expressing cells recapitulated the phenotype of *Cbfb*$^{f/f}$ NKp46-Cre mice. The number and frequency of NKp46$^+$ ILC3 cells were selectively decreased among ILC3 subsets in the PPs and LPLs of *Runx3*$^{f/f}$ NKp46-Cre mice compared to *Runx3*$^{+/f}$ NKp46-cre control mice (Fig. 3b,c). Intestinal ILC1 cells and NK cells in spleen, liver, salivary gland and skin were substantially reduced in *Runx3*$^{f/f}$ NKp46-Cre mice compared to *Runx3*$^{+/f}$ NKp46-cre mice, although the reduction was generally more modest than that observed in *Cbfb*$^{f/f}$ NKp46-Cre mice (Supplementary Fig. 1d,e; Supplementary Fig. 3a,b,c). The milder phenotype of the *Runx3*$^{f/f}$ NKp46-Cre mice compared to the *Cbfb*$^{f/f}$ NKp46-Cre mice was probably due to compensatory effects by other Runx family members, as previously described in T cell differentiation[21]. These data indicate that Runx3 is necessary for the development of ILC1 and all ILC3 subsets in the intestine.

Runx3 regulates RORγt expression in ILC3

Previous reports indicate that ILCPs express very little RORγt but express GATA-3, which is important for all ILC differentiation in the intestine[7,9]. We next investigated the hypothesis that Runx3 regulates RORγt expression in ILC3 differentiation between ILCPs and RORγt$^+$ ILC3 cells. Lin$^-$ CD127$^+$ NK1.1$^-$ LPLs are comprised of two main populations discriminated by GATA-3 and RORγt expression, GATA-3^{hi} RORγt$^-$ ILC2 cells and GATA-3^{int} RORγt$^+$ ILC3 cells (Fig. 3d), as previously described[5,15]. GATA-3^{high} ILC2 cell numbers were unaffected in the *Runx3*$^{f/f}$ Vav1-Cre mice (Fig. 3d,e), suggesting ILC2 differentiation was not abrogated by lack of Runx3 in hematopoietic cells. The overall frequencies and absolute numbers of GATA-3^{int} LPLs in adult large intestine were comparable in *Runx3*$^{f/f}$ Vav1-Cre mice and control *Runx3*$^{f/f}$ mice (Fig. 3d,e). However, in contrast to control *Runx3*$^{f/f}$ mice, the GATA-3^{int} LPLs in *Runx3*$^{f/f}$ Vav1-Cre mice did not express RORγt. These Lin$^-$ CD127$^+$ NK1.1$^-$ GATA-3^{int} RORγt$^-$ LPLs (referred to as CD127$^+$ ILCLN cells) accumulated in adult large intestine in *Runx3*$^{f/f}$ Vav1-Cre mice

compared to *Runx3*$^{f/f}$ control mice Fig. 3d.e), and were not ILCPs, because they did not express α4β7 or PLZF.

Next, we investigated if the CD127$^+$ ILCLN cells in the adult intestine have the potential to become RORγt$^+$ ILC3 cells and if Runx3 is necessary for this process. Because KLRG1 can be used as another marker for ILC2 cells among the Lin$^-$ CD127$^+$ GATA-3^{hi} cells in LPLs, we sorted Lin$^-$ CD127$^+$ α4β7$^-$ NK1.1$^-$ KLRG1$^-$ RORγt-GFP$^-$ LPLs (wild-type CD127$^+$ ILCLN cells) from adult small and large intestine of *Rorc*(γt)$^{+/GFP}$ mice (H-2^b) in which GFP is driven by *Rorc*(γt) promoter to mark ILC3 cells (Fig. 4a). Runx3-deficient CD127$^+$ ILCLN cells were sorted as Lin$^-$ CD127$^+$ α4β7$^-$ NK1.1$^-$ KLRG1$^-$ LPLs from adult small and large intestine of *Runx3*$^{f/f}$ Vav1-Cre mice without excluding RORγt$^+$ cells because RORγt$^+$ ILC3 cells were not detected in LPLs of *Runx3*$^{f/f}$ Vav1-Cre mice. The sorted cells (H-2^b) were injected into non-lethally irradiated *C. Rag2*$^{-/-}$ *Il2rg*$^{-/-}$ host mice (H-2^d). Three months after injection, donor wild-type CD127$^+$ ILCLN cells, but not Runx3-deficient CD127$^+$ ILCLN cells differentiated into intestinal Lin$^-$ CD127$^+$ GATA-3^{int} RORγt$^+$ILC3 cells (Fig. 4b). Wild-type CD127$^+$ ILCLN cells also differentiated into ILC1 cells in LPLs (Lin$^-$ CD127$^+$ NKp46$^+$ RORγt$^-$) and in IELs (Lin$^-$ CD127$^+$ NK1.1$^+$ NKp46$^+$), while ILC1 differentiation from Runx3-deficient CD127$^+$ ILCLN cells was impaired, though less than ILC3 differentiation (Fig. 4b), possibly due to compensatory effects by other Runx family members as mentioned previously. By contrast, no ILC2 cells (Lin$^-$ CD127$^+$ GATA3^{hi}) were derived from CD127$^+$ ILCLN or Runx3-deficient CD127$^+$ ILCLN cells, suggesting that CD127$^+$ ILCLN cells sorted as above are progenitor cells for ILC1 and ILC3 cells, and that Runx3 deficiency in these precursors mainly dampens differentiation to RORγt-expressing ILC3 cells.

To further confirm these findings, we cultured sorted wild-type CD127$^+$ ILCLN cells from *Rorc*(γ)t$^{+/GFP}$ mice and Runx3-deficient CD127$^+$ ILCLN cells from *Runx3*$^{f/f}$ Vav1-Cre mice on OP9-DL1 stromal cells *in vitro* with IL-2, IL-7 and stem cell factor, as previously reported[5]. On day 14, wells seeded with *Rorc*(γ)t$^{+/GFP}$ wild-type CD127$^+$ ILCLN cells contained cells which expressed RORγt-GFP (Fig. 4c), and RORγt protein expression in these cells could also be detected by anti-RORγt staining (Fig. 4d). These cells produced IL-22 in response to IL-23 and IL-1β (Fig. 4d). However, IL-22-producing, RORγt protein$^+$ cells were not detected in wells seeded with Runx3-deficient CD127$^+$ ILCLN cells (Fig. 4d). Taken together, these results indicate that expression of Runx3 is required for CD127$^+$ ILCLN cells differentiation into RORγt-expressing, IL-22-producing ILCs.

We then sought to investigate how Runx3 regulates RORγt expression in ILC3 cells. A putative Runx binding site in *Rorc*(γt) promoter was reported[25] and Runx1 regulates RORγt expression in T_H17 cells[16]. To examine if Runx3 can directly affect RORγt expression with the putative Runx-binding site in any ILC, we performed a luciferase assay with the transfectable human NK cell line NK-92 that predominately expresses Runx3 among Runx family members[26]. Transfection of the mouse RORγt promoter led to increased luciferase activity, as compared to control vector without RORγt promoter (Fig. 4e). Deletion of a Runx-binding motif in the RORγt promoter abrogated the enhanced luciferase activity (Fig. 4e). Transfection of mouse Runx3 in the NK-92 cells further increased the luciferase activity of the intact RORγt reporter, indicating that endogenous human Runx3 and ectopically

expressed mouse Runx3 can promote RORγt expression in a Runx3-binding motif-specific manner. Furthermore, using chromatin immunoprecipitation (ChIP) we detected Runx3 binding to the RORγt promoter in ILC3 cells (Fig. 4f), while Runx3 did not bind in the IL-4 promoter in ILC3 cells, as previously shown in $CD8^+$ T cells[27]. These data suggest that Runx3 directly regulates RORγt expression in ILC3 cells.

To examine if RORγt deficiency causes accumulation of $CD127^+$ ILCLN cells in adult large intestine as observed in $Runx3^{f/f}$ Vav1-Cre mice, we analyzed intestinal LPLs of $Rorc(\gamma t)^{GFP/GFP}$ (RORγt-deficient) mice. However, for reasons as yet unclear, the frequency of $CD127^+$ ILCLN cells in intestinal LPLs was comparable between wild-type and RORγt-deficient mice (Supplementary Fig. 4a). It is possible that complete deletion of RORγt in $CD127^+$ ILCLN cells might not allow the cell to survive and the low residual RORγt might be required for the accumulation of the $CD127^+$ ILCLN cells in $Runx3^{f/f}$ Vav1-Cre mice.

Because RORγt is also required for the emergence and function of LTi cells in the fetal intestine[2,28–30], we tested the effect of Runx3 deficiency on these cells. The frequencies and numbers of LTi0 ($CD3^-$ $CD11c^-$ $CD127^+$ $CD4^-$) and LTi4 ($CD3^-$ $CD11c^-$ $CD127^+$ $CD4^+$) cells[30] were comparable in $Runx3^{f/f}$ Vav1-Cre mice and $Runx3^{f/f}$ control mice. However, RORγt expression was lower in LTi cells from $Runx3^{f/f}$ Vav1-Cre mice compared to wild-type LTi cells (Supplementary Fig. 4b,c), which may explain the partial reduction of PPs in the intestine of adult $Runx3^{f/f}$ Vav1-Cre mice. These observations suggest that RORγt expression may be differentially regulated in fetal LTi cells compared to adult ILC3 cells.

T-bet is also involved in differentiation of ILC3 as well as ILC1 cells because DN ILC3 cells give rise to $NKp46^+$ ILC3 cells in a T-bet-dependent manner[13,24]. We investigated if T-bet expression was altered by Runx3 deficiency in $NKp46^+$ ILC3 cells in $Cbfb^{f/f}$ NKp46-Cre mice, which were used instead of $Runx3^{f/f}$ NKp46-Cre mice to exclude possible compensatory effects by other Runx family members. We could not obtain a large enough number of $ROR\gamma t^+$ $NKp46^+$ ILC3 cells from $Cbfb^{f/f}$ NKp46-Cre mice for analysis. However, some Lin^- $CD127^+$ $NK1.1^-$ $GATA\text{-}3^{int}$ $ROR\gamma t^{lo}$ LPLs were $NKp46^+$ in $Cbfb^{f/f}$ NKp46-Cre mice (Supplementary Fig. 5a), possibly suggesting that CBF-β deficiency might abrogate RORγt expression in $NKp46^+$ ILC3 cells. T-bet expression in these $Cbfb^{f/f}$ NKp46-Cre $GATA\text{-}3^{int}$ $ROR\gamma t^{lo}$ $NKp46^+$ cells was comparable to that in $NKp46^+$ ILC3 cells in $Cbfb^{+/f}$ NKp46-Cre control mice (Supplementary Fig. 5b). In addition, the few residual ILC1 cells in $Cbfb^{f/f}$ NKp46-Cre mice expressed T-bet normally (Supplementary Fig. 5b), suggesting that Runx3 is necessary for ILC1 and $NKp46^+$ ILC3 cells through a T-bet-independent mechanism. Taken altogether, Runx3 regulates ILC3 differentiation by inducing RORγt.

AHR expression is downstream of Runx3 in ILC3

Because AHR is a transcription factor that critically regulates ILC3 differentiation in the intestine[12,13], we next examined whether Runx3 deficiency affects AHR expression in Lin^- $CD127^+$ $NK1.1^-$ LPLs, which include ILC2, ILC3 and $CD127^+$ ILCLN cells in $Runx3^{f/f}$ mice, and ILC2 and $CD127^+$ ILCLN cells in $Runx3^{f/f}$ Vav1-Cre mice. *Ahr* as well as *Rorc*(γ)t mRNA expression was not detected in Lin^- $CD127^+$ $NK1.1^-$ LPLs isolated from $Runx3^{f/f}$ Vav1-Cre mice, which include ILC2 and $CD127^+$ ILCLN cells (Fig. 4g). In

contrast, *Runx3*$^{f/f}$ Vav1-Cre Lin^{-} CD127^{+} NK1.1^{-} cells had higher expression of *Gata3* than *Runx3*$^{f/f}$ control mice, similar to observations made in Runx3-deficient CD8^{+} T cells[31]. These data suggest that AHR is downstream of Runx3 in ILC3 development.

To test if Runx3 controlled *AhR* expression directly or indirectly, through controlling the expression of RORγt, we determined *Ahr* mRNA expression in Lin^{-} CD127^{+} NK1.1^{-} LPLs from small and adult intestine of *Rorc*(γt)$^{+/GFP}$ mice, which are heterozygous for *RORγt* expression. RT-PCR analysis showed a 50% reduction in *Ahr* mRNA expression in *Rorc*(γt)$^{+/GFP}$ Lin^{-} CD127^{+} NK1.1^{-} LPLs compared to wild-type (Supplementary Fig. 6a), suggesting that AHR is downstream of RORγt in ILC3 cells. To determine if RORγt can bind either to the *Ahr* promoter or enhancers, we used published RORγt ChIP-seq data[32] as well as histone acetyltransferase p300 and H3K4 dimethylation (H3K3me2) profiles from T_H17 cells (Supplementary Fig. 6b), which express RORγt and AHR similar to ILC3 cells. The alignment of these data sets indicated that RORγt binds to at least three sites in the vicinity of *Ahr* transcription start site, which according to their H3K4me2 modification and p300 binding, could be *Ahr* enhancer regions (Supplementary Fig. 6b). These data are consistent with the possibility that RORγt directly regulates *Ahr* via enhancer interactions.

To assess the possibility of direct regulation, we investigated the binding of Runx3 to the *Ahr* promoter in splenic NK cells, which express both Runx3 and AHR[18,33]. Published ChIP-seq data showed that active promoter or enhancer regions of *Ahr* promoter marked by H3K4 mono-methylation in splenic NK cells were almost identical to those marked by H3K4 di-methylation in T_H17 cell[18] (Supplementary Fig. 6b). However, Runx3 binding was not detected in the *Ahr* promoter or enhancers in splenic NK cells (Supplementary Fig. 6b), indicating that Runx3 does not regulate AHR in NK cells, and could be taken as an indication that *Ahr* is also not directly regulated by Runx3 in ILC3 cells. Collectively, these data suggest that AHR expression is regulated by RORγt, whose expression is under direct control of Runx3 in ILC3s.

Runx3 is required for survival of ILC1 but not ILC3

In splenic NK cells, Runx3 regulates the expression of genes related to cell survival and proliferation downstream of IL-15 signaling[18]. Because IL-15 acts as a survival factor for splenic NK cells and intestinal ILC1 cells[5,8,23] we examined whether Runx3 controls survival of ILC1 cells in intestine. The residual intestinal ILC1 cells and liver-resident DX5^{-} CD49a^{+} NK cells in the *Cbfb*$^{f/f}$ NKp46-Cre and *Runx3*$^{f/f}$ NKp46-Cre mice were more apoptotic (as assessed by Annexin V staining) and had higher proliferation (as assessed by Ki67 staining) than those in *Cbfb*$^{+/f}$ NKp46-Cre and *Runx3*$^{+/f}$ NKp46-Cre control mice (Fig. 5a,b and Supplementary Fig. 7a,b). However, the effect of Runx3 deletion among various ILC1 subsets varied somewhat because of apparent tissue-dependent effects. For example, *Runx3*$^{f/f}$ NKp46-Cre NK cells in spleen and salivary gland had normal or only marginally increased apoptosis compared to control *Runx3*$^{+/f}$ NKp46-Cre NK cells, while showing increased proliferation compared to control *Runx3*$^{+/f}$ NKp46-Cre NK cells (Supplementary Fig. 7a,b). Moreover, DX5^{+} CD49a^{-} liver NK cells are thought to correspond to splenic NK cells, because they share the same gene expression profiles, trafficking properties and transcription factor dependence[23]. However, *Cbfb*$^{f/f}$ NKp46-Cre and *Runx3*$^{f/f}$ NKp46-Cre

DX5$^+$ CD49a$^-$ liver NK cells show less pronounced annexin V staining compared to their spleen counterparts (Supplementary Fig. 7a). Regardless, ILC1 cells in the intestine show enhanced apoptosis in the absence of CBF-β and Runx3.

To explore the mechanism of Runx-dependent apoptosis, we examined the expression of regulators of apoptosis in *Cbfb*$^{f/f}$ NKp46-Cre ILC1 cells. Bcl-2 is induced by IL-15 stimulation and involved in NK cell survival[34]. Bcl-2 expression was significantly reduced in IL-15-stimulated intestinal *Cbfb*$^{f/f}$ NKp46-Cre ILC1 cells compared to *Cbfb*$^{+/f}$ NKp46-Cre control ILC1 cells (Fig. 5c). In addition, CBF-β or Runx3 deficiency in ILC1 cells led to increased total caspase activity compared to *Cbfb*$^{+/f}$ NKp46-Cre control ILC1 cells (Fig. 5d). Therefore, Runx3 may control the survival of ILC1 cells through regulating the expression of anti-apoptotic genes, including Bcl-2.

To determine whether CBF-β and Runx3 also control the survival of ILC3 cells, we used PP lymphocytes instead of LPLs, because the collagenase treatments used to isolate LPLs caused cell death and interfered with the apoptosis assay. NKp46$^+$ Lin$^-$ CD127$^+$ NK1.1$^-$ GATA-3^{int} cells from *Cbfb*$^{f/f}$ NKp46-Cre mice, which had lost RORγt expression, had similar apoptosis rates compared to NKp46$^+$ ILC3 cells from *Cbfb*$^{+/f}$ NKp46-Cre mice (Fig. 5e). In addition, *Runx3*$^{f/f}$ Vav1-Cre Lin$^-$ CD127$^+$ NK1.1$^-$ GATA-3^{int} cells, which cannot express RORγt because of their Runx3 deficiency, did not show increased apoptotic rates compared to *Runx3*$^{+/f}$ Lin$^-$ CD127$^+$ NK1.1$^-$ GATA-3^{int} cells (Fig. 5f). These data imply that CBF-β and Runx3 are crucial for the survival of ILC1 but not ILC3 in the intestine.

Cell-intrinsic role of Runx3 for ILC1 and ILC3 in intestine

Because crosstalks between innate lymphocytes and CD4$^+$ T cells have been described[35,36] and CD4$^+$ T lineage commitment was also affected in *Runx3*$^{f/f}$ Vav1-Cre mice, we tested whether Runx3 deficiency affected ILC numbers via cell-intrinsic or cell-extrinsic effects. We generated competitive bone marrow chimeric mice by transferring *Cbfb*$^{+/f}$ NKp46-Cre, *Cbfb*$^{f/f}$ NKp46-Cre, *Runx3*$^{f/f}$ or *Runx3*$^{f/f}$ Vav1-Cre bone marrow cells (Ly5.2$^+$) mixed in equal ratios (1:1) with wild-type bone marrow cells (Ly5.1$^+$) into lethally-irradiated Ly5.1$^+$ congenic mice. Donor chimerism was examined 8–10 weeks post injection in spleen and intestinal PPs, IELs and LPLs based on Ly5.1 and Ly5.2 expression. Less ILC1 and NKp46$^+$ ILC3 cells were derived from *Cbfb*$^{f/f}$ NKp46-Cre donor cells (Fig. 6a) and *Runx3*$^{f/f}$ Vav1-Cre donor cells (Fig. 6b) compared to the wild-type competitor cells, demonstrating the importance of intrinsic Runx3 in the development or maintenance of ILC1 and ILC3 cells in the intestine. In particular, almost no ILC3 cells were recovered from *Runx3*$^{f/f}$ Vav1-Cre donor bone marrow in PPs (Fig. 6b). On the other hand, *Runx3*$^{f/f}$ Vav1-Cre derived ILC2 cells repopulated the intestinal lamina propria and PPs to the same extent as wild-type cells. Thus, Runx3 deficiency affects the development or maintenance of ILC1 and ILC3 cells in a cell-intrinsic manner, but does not affect ILC2 cells.

Runx3 in ILCs is essential for protection against *C. rodentium*

We next determined the physiological role of Runx3 expression in ILCs using a model of *C. rodentium* infection in *Runx3*$^{f/f}$ NKp46-Cre mice, considering that CD4$^+$ T cells[37], other hematopoietic cells and enterocytes[38] also could be affected in *Runx3*$^{f/f}$ Vav1-Cre mice.

Runx3$^{f/f}$ NKp46-Cre infected mice showed a similar degree of body weight loss and survival compared to *Runx3*$^{+/f}$ NKp46-Cre mice (data not shown), similar to observations made in T-bet-deficient mice, which do not have intestinal ILC1 and NKp46^{+} ILC3 cells[4,24]. However, on day 8 after infection with *C. rodentium*, *Runx3*$^{f/f}$ NKp46-Cre mice had shorter colon lengths and higher bacterial titers in the spleen than *Runx3*$^{+/f}$ NKp46-Cre control mice (Fig. 7a,b). Compared to uninfected *Runx3*$^{wt/f}$ NKp46-Cre control mice, there was similarly no inflammation in the *Runx3*$^{f/f}$ NKp46-Cre mice without *C. rodentium* infection (Fig. 7c). However, following infection, *Runx3*$^{f/f}$ NKp46-Cre mice had more persistent intestinal damage including features of increased epithelial injury, crypt hyperplasia and increased inflammatory cell infiltration compared to *Runx3*$^{f/f}$ NKp46-Cre control mice (Fig. 7c, d). These observations suggest a specific role for ILC1 and NKp46^{+} ILC3 cells in controlling *C. rodentium* infection.

Because IL-22, especially from ILC3 cells, and IFN-γ are required to control acute infection with *C. rodentium*[3,13,24,39], we examined the production of these cytokines in *C. rodentium*–infected *Runx3*$^{f/f}$ NKp46-Cre mice. IL-22-producing ILC3 cells were strongly reduced in the intestine of these mice (Fig. 7e,f). In addition, IFN-γ-producing ILC1 cells in IELs and LPLs were only scarcely detected in *Runx3*$^{f/f}$ NKp46-Cre mice after infection as compared to *Runx3*$^{f/f}$ NKp46-Cre control mice (Fig. 7g,h,i), indicating that Runx3 expression in ILCs is critical for host immunity and cytokine production against *C. rodentium* infection.

DISCUSSION

In this study, we show that Runx3 regulates the development and/or maintenance of ILC1 and ILC3 cells in the intestine. Runx3 induced the transcriptional regulator RORγt and its downstream target AHR in ILC3 cells. Runx3 regulated the differentiation of ILC3 from progenitor cells specific to ILC1 and ILC3 cells into RORγt^{+} ILC3 cells in the adult mouse intestine. As a maintenance factor, Runx3 was necessary for the survival of ILC1 cells, but not ILC3 cells. Runx3 deficiency had a limited effect on ILC1 development, probably due to compensatory effects by other Runx family members at steady-state. Competitive bone marrow chimeras revealed the cell-intrinsic contribution of Runx3 to the development of ILC1 and ILC3 cells, but not ILC2 cells. Finally, a requirement for Runx3 in the maintenance of ILCs was evident after *C. rodentium* infection. Thus, these results establish Runx3 as a key player in ILC lineage-specific differentiation.

Taken together, our data add substantial evidence supporting the parallel but somewhat distinct differentiation of ILCs and CD4^{+} T cell subsets. CD4^{+} T cells and ILCs share the same signature transcription factors, although all ILCs in the intestine differentially express GATA-3. CD127+ ILC1 and ILC3 cells also express GATA-3 at intermediate levels while ILC2 cells are characterized by high GATA-3 expression. T_H1 cells and ILC1 cells are characterized by high expression of T-bet and Runx3. T_H2 cells and ILC2 cells are identified as GATA-3^{hi} populations. T_H17 cells use Runx1 to induce RORγt expression, while in ILC3 cells RORγt is driven by Runx3. Because Runx family members orchestrate CD4^{+} T cell differentiation together with GATA-3 and T-bet, our findings offer additional insights into the mechanism of ILC lineage differentiation.

Without Runx3, ILC3 development was arrested at the CD127$^+$ ILCLN stage. GATA-3 controls CD127 expression[9] and only the PLZF$^+$ cells among Lin$^-$ CD127$^+$ bone marrow cells express distal Runx3. Although these findings suggest that Runx3 could be downstream of GATA-3, the inducible deletion of GATA-3 in ILC3 cells did not alter Runx1 and Runx3 expression[9]. The interpretation that Runx3 is not regulated by GATA-3 in ILCs is also supported by the observations that ILC2 cells do not express distal Runx3 in spite of high GATA-3 expression. GATA-3 expression is rather inversely correlated with distal Runx3 expression, because only GATA-3^{int} ILC1 and ILC3 cells, but not GATA-3^{hi} ILC2 cells, express distal Runx3.

Runx3 promotes T_H1 commitment and represses GATA-3 through direct binding to GATA-3[40]. Conversely, GATA-3 blocks Runx3 function by direct interaction with Runx3 in T_H2 cells[41], suggesting that the balance between GATA-3 and Runx3 controls the lineage determination toward T_H1 or T_H2 cells. The same transcriptional network could regulate ILC1 and ILC2 differentiation, considering that ILCPs express both GATA-3 and Runx3. ILC1 cells express high amounts of Runx3, which is apparently necessary to overcome their GATA-3 expression. By contrast, ILC2 cells acquire high GATA-3 expression and lose Runx3 expression, which appears necessary for the GATA-3-dependent machinery to drive ILCPs to ILC2 cells. Additionally, Runx family members interact with T-bet to control CD4$^+$ T cell differentiation. T-bet regulates Runx3 to enhance T_H1 commitment and attenuates T_H17 skewing by inhibiting Runx1-mediated RORγt expression through antagonistic binding to Runx1[27,42,43]. Possible interactions of T-bet with Runx3 during ILC lineage determination seem to be very complex. During ILC differentiation Runx3 expression is induced earlier than T-bet expression, because ILCPs express Runx3 but not T-bet[7]. It is not still clear how T-bet is induced, associates with Runx3 and differentially regulates two different subsets of T-bet-dependent ILCs, ILC1 and NKp46$^+$ ILC3 cells.

Prior data showed that Runx1 or CBF-β deficiency is associated with reduction of LTi cells in the fetal intestine[19]. However, it was challenging to interpret these data at that time in the absence of knowledge of ILC progenitor cells. Here we investigated the expression of Runx family members in ILC progenitor cells and all ILC subsets. Runx3, not Runx1, was mainly expressed by ILC1 and ILC3 cells and contributed to ILC lineage commitment toward these two subsets. Although Runx1 expression is not very high in CLPs, Runx1 is critical for differentiation of Flt3$^+$ progenitor cells including CLPs[17]. Runx1 may also have a critical role in ILC differentiation along with Runx3, just before ILC lineage commitment, because both Runx1 and Runx3 were highly expressed in ILCPs. Further studies will be required to determine the function of Runx1 and Runx3 in ILCPs.

RORγt expression was less severely affected in Runx3-deficient fetal LTi cells than in adult ILC3 cells. This could be due to different requirements for their development[29,44,45] and/or to different compensatory effects. For example, IL-15 or IL-2 stimulation is required to reveal proliferation defects in splenic NK cells lacking Runx3[18]. Also, the reduction of ILC1 cells in Runx3-deficient mice was more evident in *C. rodentium*-infected *Runx3*$^{f/f}$ NKp46-Cre mice. Thus, differences in microbiota or inflammatory circumstances in fetal versus adult intestine may affect the Runx3 requirement for RORγt expression in ILC3 cells.

The CD127$^+$ ILCLN cell described here in *Runx3*$^{f/f}$ Vav1-Cre mice are α4β7-negative. By contrast, some studies found ILC progenitor cells in the Lin$^-$ CD127$^+$ α4β7$^+$ population from BM, fetal liver and intestine[5,7,44,46]. However, it should be noted that adult ILCs in the intestine do not express α4β7, but do express CD127[7,10] (data not shown)[7,10]. Therefore, the CD127$^+$ ILCLN cells described here could be ILC1- and ILC3-specific ILC progenitors that have already migrated to the intestine, but were arrested in their ILC3 development because they require Runx3 and RORγt for further differentiation.

Runx3 dysfunction has been discussed for many years in the pathogenesis of colitis[37,47,48]. Aberrant T_H17 cells deficient for Runx3 were reported to be sufficient to induce colitis[37]. Herein, we demonstrated that Runx3 is indispensable to development of ILC3 cells, which are main source of IL-22 in intestine to maintain epithelial integrity. Thus, Runx3 mutations and loss of Runx3 function can dampen the host's ability to protect the intestinal barrier against microbes, implicating Runx3 defects in the pathogenesis of intestinal inflammation.

METHODS

Mice

All the mice were bred and maintained at a specific pathogen-free facility of Washington University School of Medicine and animal protocols were approved by the Washington University Animal Studies Committee. C57BL/6 mice and congenic Ly5.1$^+$mice were obtained from NCI. *Rorc*(γt)$^{+/GFP}$ and *Vav1*-Cre transgenic mice were obtained from Jackson. *Cbfb*$^{f/f}$, *Runx3*$^{f/f}$, *Runx3d*$^{+/YFP}$ mice were previously described[22] and provided by Dan R. Littman (New York University, New York, NY). NKp46-Cre mice were kindly provided by Eric Vivier[49] (Centre d'Immunologie de Marseille-Luminy, Marseille, France). All Cre mice were heterozygous. Control mice were all littermates.

Cell preparation

Lymphocytes from the small and large intestine were isolated as previously described[8,13] with some modifications. Briefly, small and large intestines were dissected and fat tissues were removed. Peyer's patches were removed from the small intestine and smashed through 70μm strainer. Intestines were cut open longitudinally, washed with PBS then cut into 5 mm-length pieces, followed by incubation with HBSS buffer including 10% FBS, 5mM EDTA and 15mM HEPES at 37 °C for 20 min. After being vortexed for 20s, the dissociated cells were collected for intra epithelial lymphocytes. To isolate lamina propria cells, rest of the tissues were washed with PBS twice and 0.5 g of the tissues were digested with 25 ml of RPMI1640 media including 5 mg of Liberase TL (Roche Life Sciences), 5 mg of DNase I (Roche) and 50 mg of Dispase II (Roche) at 37 °C for 30 min. The digested tissues were passed through 100 μm and 70 μm strainer after vigorous vortexing for 20s. Then, lymphocytes were isolated from the interphase of 40 % and 80 % Percoll gradient after centrifugation at 1800 rpm for 20 min.

Antibodies and flow cytometry

Supernatant of hybridoma 2.4g2 (anti-CD16/32) was used to block Fc receptor. Cells were stained with Fixable Viability Dye eFluor 506 (eBioscience) to detect dead cells before

surface staining. Annexin V apoptosis detection kit, eFlour 450 (eBioscience) and Ki-67 kit (BD Biosciences) were used according to manufacturers' protocol. Antibodies used for flow cytometry were listed in Supplementary Table 1. Pan-caspase activity was detected by FAM-FLICA™ Poly Caspase Assay Kit (ImmunoChemistry Technologies) according to manufacturer's protocol. For intracellular cytokine staining and transcription factor staining, Foxp3/Transcription Factor Staining Buffer Set (eBioscience) was used as manufacturer's protocol. IELs (1×10^6 cells/ml) and LPLs (1×10^6 cells/ml) were stimulated with IL-12 (10 ng/mL) or IL-23 (10ng/mL)/IL-1β (10ng/mL) with GolgiPlug at 37°C for 4 hours for cytokine production, or IL-15 (20 ng/mL) at 37°C for 24 hours for Bcl-2 expression. Data were acquired on a FACSCanto II (BD Biosciences) and analyzed with FlowJo software (TreeStar).

RT-PCR

ILC1 cells from IELs, ILC3 subsets from LPLs and $CD45^+$ $CD3^-$ $CD19^-$ $CD127^+$ $NK1.1^-$ LPLs were isolated from small and large intestines and sorted by Moflo. CLPs, αLPs, CHILP, ILCPs, ILC2P were isolated from bone marrow cells. RNA was purified with Trizol (Life technologies) and cDNA was synthesized with Superscript III First Strand Synthesis Kit (Life technologies) according to manufacturer's protocol. Then, mRNA transcripts were quantified with a StepOnePlus Real-Time PCR System and iQ SYBR Green Supermix (Biorad). The absolute expression of *CBFβ, Runx1, Runx2* and *Runx3* (standard curve method) and the relative expression of *Blimp1, GATA-3, RORγt* and *AHR* ($2^{-\text{deltaCt}}$ method) were calculated and normalized to *Actb* expression. For RT-PCR to detect distal and proximal Runx3, normalized amount of cDNA was applied to PCR (Advantage GC2 PCR kit; Clontech). Specific primers were listed in Supplementary Table 2.

In vitro ILC differentiation and adoptive transfer

In vitro cell culture to support all ILC differentiation was reported elsewhere[5]. Briefly, $CD45^+$ $CD3^-$ $CD19^-$ $CD127^+$ $\alpha4\beta7^-$ $NK1.1^-$ $KLRG1^-$ $ROR\gamma t^-$ or $ROR\gamma t^+$ cells from *Rorc*$(\gamma t)^{+/GFP}$ mice and $CD45^+$ $CD3^-$ $CD19^-$ $CD127^+$ $\alpha4\beta7^-$ $NK1.1^-$ $KLRG1^-$ cells from *Runx3*$^{f/f}$ Vav1-Cre mice were sorted by Moflo. Then, 2.000 to 10.000 cells were injected into *C. Rag2*$^{-/-}$ *Il2gc*$^{-/-}$ mice irradiated at 450 rad or 100 cells were cultured in individual wells containing a monolayer of mitomycin C-treated OP9-DL1 cells with IL-7 (25ng/mL), SCF (25ng/mL) and IL-2 (10ng/mL) for 14 days. Cultured cells were stimulated with IL-23 (30 ng/ml) and IL-1β (30 ng/ml) with GolgiPlug at 37°C for 4 hours to induce IL-22 production.

Luciferase assay

The RORγt promoter encompassing a region from −242 to +109 relative to the transcription start site was inserted into the Xho1/HindIII site of pGL3. To mutate the Runx binding motif, TGTGGTT (nt −174 to −168 from the transcription start site), we modified it to TACAATT. NK-92 cells were obtained from ATCC and transfected with Amaxa cell line Nucleofector Kit R (Lonza) by manufacturer's protocol. Briefly, 5×10^6 cells of NK-92 cells were electroporated with 1 μg of pGL3 vector with 1 μg of empty pEF vector or Runx3-pEF vector. After 18 hour incubation at 37°C, 5 % CO_2, the cells were harvested,

counted for normalization and resuspended in Glo Lysis Buffer. Luciferase activity was measured by 1450 Micro Beta (Wallac).

Chromatin immunoprecipitation

ILC3 cells (1.5×10^5 cells) were isolated from *Rorc*$(\gamma t)^{+/GFP}$ mice. Cells were cross-linked with 1% paraformaldehyde, lysed and sonicated to generate 100–300 bp DNA fragments. DNA prepared from 5% of sample prior to immunoprecipitation was used as input DNA. DNA-protein complexes were immunoprecipitated with 4μl of rabbit anti-Runx3 sera, developed in the Groner lab[18]. After reverse-cross-linking and DNA purification, immunoprecipitated DNA fragments were analyzed by qRT-PCR using SYBR green. Primers were listed in Supplementary Table 2.

Generation of bone marrow chimeras

Congenic Ly5.1$^+$ mice were lethally irradiated at 950 rad and reconstituted with 1×10^7 cells of Ly5.1$^+$ WT bone marrow cells and 1×10^7 cells of Ly5.2$^+$ bone marrow cells which were obtained from *Cbfb*$^{+/f}$ NKp46-Cre, *Cbfb*$^{f/f}$ NKp46-Cre, *Runx3*$^{f/f}$ or Runx3$^{f/f}$ Vav1-Cre mice. After 8–10 weeks, spleen, PPs, IELs and LPLs in small and large intestine were collected for analysis.

C. rodentium infection

Runx3$^{+/f}$ NKp46-Cre or *Runx3*$^{f/f}$ NKp46-Cre mice were orally infected with 5×10^9 *C. rodentium* strain DBS100 (American Type Culture Collection) as described elsewhere[13]. On day 8 after infection, spleen, small intestine and colon were harvested from the infected mice. Spleens were weighed, transferred into a 2 ml tube with 1ml of PBS and a 5 mm metal bead (Qiagen) and homogenized with Mini-BeadBeater-8 (Biospec) at a medium speed for one minute. One hundred μl of homogenates were plated onto MacConkey agar plates and *C. rodentium* colonies were counted after overnight incubation at 37°C. Colon was fixed with Methacarn at 4°C for 2 hours, then 70% ethanol at 4°C for 1 hour, incubated with 20% sucrose in PBS overnight and embedded into OCT compound (Tissue-Tek) for HE-staining. Colons were used to isolate IELs and LPLs as describe above. To examine colonic pathology based on a previously published pathology scoring system[50], observers were blinded to the experimental conditions. The pathological parameters include 1) the extent of inflammatory infiltration 2) degree of epithelial hyperplasia 3) goblet cell depletion and 4) crypt abscess. Data are represented as the percentage of damaged area along the colonic tissue.

Statistical analyses

Data were analyzed by two-tailed Student's *t*-test with Graphpad Prizm 4. *P* values of <0.05 considered statistically significant. No randomization was used in animal studies. No deliberate attempt was made to study only selected mice except based on genotype. No blinding was done except for histological scoring.

Supplementary Material

Refer to Web version on PubMed Central for supplementary material.

ACKNOWLEDGMENTS

We thank E. Vivier and D.R. Littman for mice; S. Taffner for technical assistance; H. Miyoshi and A. Fuchs for technical advice; and D.K. Sojka, and S. Demehri for helpful discussion. This study was supported by the Howard Hughes Medical Institute (W.M.Y.) and the US National Institutes of Health (R01AI097244 to T.Eg.). M.D.B. is supported by NIH training grant T32-GM007200.

References

1. Diefenbach A, Colonna M, Koyasu S. Development, Differentiation, and Diversity of Innate Lymphoid Cells. Immunity. 2014; 41:354–365. [PubMed: 25238093]
2. Eberl G, et al. An essential function for the nuclear receptor RORgamma(t) in the generation of fetal lymphoid tissue inducer cells. Nat Immunol. 2004; 5:64–73. [PubMed: 14691482]
3. Satoh-Takayama N, et al. Microbial flora drives interleukin 22 production in intestinal NKp46+ cells that provide innate mucosal immune defense. Immunity. 2008; 29:958–970. [PubMed: 19084435]
4. Klose CS, et al. A T-bet gradient controls the fate and function of CCR6-RORgammat+ innate lymphoid cells. Nature. 2013; 494:261–265. [PubMed: 23334414]
5. Klose CS, et al. Differentiation of type 1 ILCs from a common progenitor to all helper-like innate lymphoid cell lineages. Cell. 2014; 157:340–356. [PubMed: 24725403]
6. Yu X, et al. The basic leucine zipper transcription factor NFIL3 directs the development of a common innate lymphoid cell precursor. Elife. 2014; 3
7. Constantinides MG, McDonald BD, Verhoef PA, Bendelac A. A committed precursor to innate lymphoid cells. Nature. 2014; 508:397–401. [PubMed: 24509713]
8. Fuchs A, et al. Intraepithelial type 1 innate lymphoid cells are a unique subset of IL-12- and IL-15-responsive IFN-gamma-producing cells. Immunity. 2013; 38:769–781. [PubMed: 23453631]
9. Yagi R, et al. The transcription factor GATA3 is critical for the development of all IL-7Ralpha-expressing innate lymphoid cells. Immunity. 2014; 40:378–388. [PubMed: 24631153]
10. Hoyler T, et al. The transcription factor GATA-3 controls cell fate and maintenance of type 2 innate lymphoid cells. Immunity. 2012; 37:634–648. [PubMed: 23063333]
11. Halim TY, et al. Retinoic-acid-receptor-related orphan nuclear receptor alpha is required for natural helper cell development and allergic inflammation. Immunity. 2012; 37:463–474. [PubMed: 22981535]
12. Qiu J, et al. The aryl hydrocarbon receptor regulates gut immunity through modulation of innate lymphoid cells. Immunity. 2012; 36:92–104. [PubMed: 22177117]
13. Lee JS, et al. AHR drives the development of gut ILC22 cells and postnatal lymphoid tissues via pathways dependent on and independent of Notch. Nat Immunol. 2012; 13:144–151. [PubMed: 22101730]
14. Basu R, Hatton RD, Weaver CT. The Th17 family: flexibility follows function. Immunol Rev. 2013; 252:89–103. [PubMed: 23405897]
15. Serafini N, et al. Gata3 drives development of RORgammat+ group 3 innate lymphoid cells. J Exp Med. 2014; 211:199–208. [PubMed: 24419270]
16. Wong WF, Kohu K, Chiba T, Sato T, Satake M. Interplay of transcription factors in T-cell differentiation and function: the role of Runx. Immunology. 2011; 132:157–164. [PubMed: 21091910]
17. Satpathy AT, et al. Runx1 and Cbfbeta regulate the development of Flt3+ dendritic cell progenitors and restrict myeloproliferative disorder. Blood. 2014; 123:2968–2977. [PubMed: 24677539]
18. Levanon D, et al. Transcription factor Runx3 regulates interleukin-15-dependent natural killer cell activation. Mol Cell Biol. 2014; 34:1158–1169. [PubMed: 24421391]
19. Tachibana M, et al. Runx1/Cbfbeta2 complexes are required for lymphoid tissue inducer cell differentiation at two developmental stages. J Immunol. 2011; 186:1450–1457. [PubMed: 21178013]

20. Pozner A, et al. Transcription-coupled translation control of AML1/RUNX1 is mediated by cap- and internal ribosome entry site-dependent mechanisms. Mol Cell Biol. 2000; 20:2297–2307. [PubMed: 10713153]
21. Egawa T, Tillman RE, Naoe Y, Taniuchi I, Littman DR. The role of the Runx transcription factors in thymocyte differentiation and in homeostasis of naive T cells. J Exp Med. 2007; 204:1945–1957. [PubMed: 17646406]
22. Egawa T, Littman DR. ThPOK acts late in specification of the helper T cell lineage and suppresses Runx-mediated commitment to the cytotoxic T cell lineage. Nat Immunol. 2008; 9:1131–1139. [PubMed: 18776905]
23. Sojka DK, et al. Tissue-resident natural killer (NK) cells are cell lineages distinct from thymic and conventional splenic NK cells. Elife. 2014; 3:e01659. [PubMed: 24714492]
24. Rankin LC, et al. The transcription factor T-bet is essential for the development of NKp46+ innate lymphocytes via the Notch pathway. Nat Immunol. 2013; 14:389–395. [PubMed: 23455676]
25. Xi H, Schwartz R, Engel I, Murre C, Kersh GJ. Interplay between RORgammat, Egr3, and E proteins controls proliferation in response to pre-TCR signals. Immunity. 2006; 24:813–826. [PubMed: 16782036]
26. Lai CB, Mager DL. Role of runt-related transcription factor 3 (RUNX3) in transcription regulation of natural cytotoxicity receptor 1 (NCR1/NKp46), an activating natural killer (NK) cell receptor. J Biol Chem. 2012; 287:7324–7334. [PubMed: 22253448]
27. Cruz-Guilloty F, et al. Runx3 and T-box proteins cooperate to establish the transcriptional program of effector CTLs. J Exp Med. 2009; 206:51–59. [PubMed: 19139168]
28. Sun Z, et al. Requirement for RORgamma in thymocyte survival and lymphoid organ development. Science. 2000; 288:2369–2373. [PubMed: 10875923]
29. Sawa S, et al. Lineage relationship analysis of RORgammat+ innate lymphoid cells. Science. 2010; 330:665–669. [PubMed: 20929731]
30. van de Pavert SA, et al. Maternal retinoids control type 3 innate lymphoid cells and set the offspring immunity. Nature. 2014; 508:123–127. [PubMed: 24670648]
31. Lotem J, et al. Runx3-mediated transcriptional program in cytotoxic lymphocytes. PLoS One. 2013; 8:e80467. [PubMed: 24236182]
32. Ciofani M, et al. A validated regulatory network for Th17 cell specification. Cell. 2012; 151:289–303. [PubMed: 23021777]
33. Shin JH, et al. Modulation of natural killer cell antitumor activity by the aryl hydrocarbon receptor. Proc Natl Acad Sci U S A. 2013; 110:12391–12396. [PubMed: 23836658]
34. Cooper MA, et al. In vivo evidence for a dependence on interleukin 15 for survival of natural killer cells. Blood. 2002; 100:3633–3638. [PubMed: 12393617]
35. Gasteiger G, Rudensky AY. Interactions between innate and adaptive lymphocytes. Nat Rev Immunol. 2014; 14:631–639. [PubMed: 25132095]
36. Hepworth MR, Sonnenberg GF. Regulation of the adaptive immune system by innate lymphoid cells. Curr Opin Immunol. 2014; 27:75–82. [PubMed: 24594491]
37. Reis BS, Rogoz A, Costa-Pinto FA, Taniuchi I, Mucida D. Mutual expression of the transcription factors Runx3 and ThPOK regulates intestinal CD4(+) T cell immunity. Nat Immunol. 2013; 14:271–280. [PubMed: 23334789]
38. Liu JY, et al. Vav proteins are necessary for correct differentiation of mouse cecal and colonic enterocytes. J Cell Sci. 2009; 122:324–334. [PubMed: 19139088]
39. Simmons CP, et al. Impaired resistance and enhanced pathology during infection with a noninvasive, attaching-effacing enteric bacterial pathogen, Citrobacter rodentium, in mice lacking IL-12 or IFN-gamma. J Immunol. 2002; 168:1804–1812. [PubMed: 11823513]
40. Kohu K, et al. The Runx3 transcription factor augments Th1 and down-modulates Th2 phenotypes by interacting with and attenuating GATA3. J Immunol. 2009; 183:7817–7824. [PubMed: 19933870]
41. Yagi R, et al. The transcription factor GATA3 actively represses RUNX3 protein-regulated production of interferon-gamma. Immunity. 2010; 32:507–517. [PubMed: 20399120]

42. Lazarevic V, et al. T-bet represses T(H)17 differentiation by preventing Runx1-mediated activation of the gene encoding RORgammat. Nat Immunol. 2011; 12:96–104. [PubMed: 21151104]
43. Djuretic IM, et al. Transcription factors T-bet and Runx3 cooperate to activate Ifng and silence Il4 in T helper type 1 cells. Nat Immunol. 2007; 8:145–153. [PubMed: 17195845]
44. Possot C, et al. Notch signaling is necessary for adult, but not fetal, development of RORgammat(+) innate lymphoid cells. Nat Immunol. 2011; 12:949–958. [PubMed: 21909092]
45. Sanos SL, et al. RORgammat and commensal microflora are required for the differentiation of mucosal interleukin 22-producing NKp46+ cells. Nat Immunol. 2009; 10:83–91. [PubMed: 19029903]
46. Cherrier M, Sawa S, Eberl G. Notch, Id2, and RORgammat sequentially orchestrate the fetal development of lymphoid tissue inducer cells. J Exp Med. 2012; 209:729–740. [PubMed: 22430492]
47. Brenner O, et al. Loss of Runx3 function in leukocytes is associated with spontaneously developed colitis and gastric mucosal hyperplasia. Proc Natl Acad Sci U S A. 2004; 101:16016–16021. [PubMed: 15514019]
48. Weersma RK, et al. Runt-related transcription factor 3 is associated with ulcerative colitis and shows epistasis with solute carrier family 22, members 4 and 5. Inflamm Bowel Dis. 2008; 14:1615–1622. [PubMed: 18668679]
49. Narni-Mancinelli E, et al. Fate mapping analysis of lymphoid cells expressing the NKp46 cell surface receptor. Proc Natl Acad Sci U S A. 2011; 108:18324–18329. [PubMed: 22021440]
50. Brown JB, et al. Epithelial phosphatidylinositol-3-kinase signaling is required for beta-catenin activation and host defense against Citrobacter rodentium infection. Infect Immun. 2011; 79:1863–1872. [PubMed: 21343355]

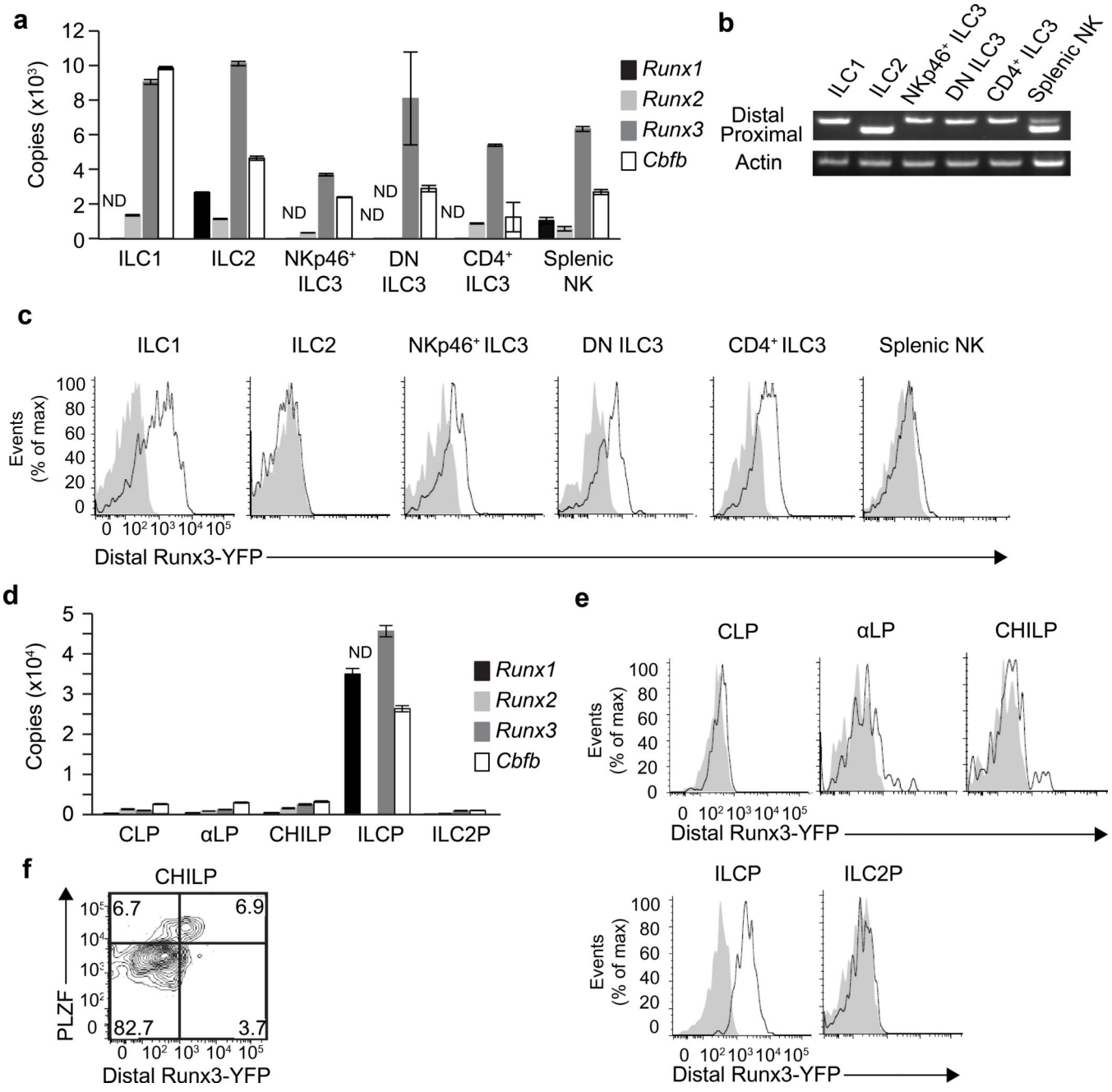

Figure 1.

ILC1 and all ILC3 subsets predominantly express Runx3 from the distal promoter. (**a, b, d**) Quantitative RT-PCR (a, d) and RT-PCR (b) analysis showing expression of indicated genes in intestinal ILC1 cells ($CD45^+$ $CD3^-$ $CD19^-$ $NK1.1^+$ $NKp46^+$ $CD49a^+$), intestinal ILC2 cells ($CD45^+$ $CD3^-$ $CD19^-$ $CD127^+$ $KLRG1^+$ $CD25^+$) and splenic NK cells ($CD3^-$ $CD19^-$ $NK1.1^+$ $NKp46^+$) from wild-type (WT) mice; in intestinal ILC3 subsets ($CD45^+$ $CD3^-$ $CD19^-$ $CD127^+$ GFP^+) from *Rorc*$(\gamma t)^{+/GFP}$ mice; in common lymphoid progenitor cells (CLP: $CD45^+$ Lin^- $cKit^{lo}$ $CD127^+$ $sca1^{lo}$ $Flt3^+$ $\alpha4\beta7^-$), $\alpha4\beta7$ integrin-expressing CLP (αLP: $CD45^+$ Lin^- $cKit^{lo}$ $CD127^+$ $sca1^{lo}$ $Flt3^-$ $\alpha4\beta7^+$), common progenitor to all helper-like innate

lymphoid cell lineages (CHILP: $CD45^+$ Lin^- $CD127^+$ $\alpha4\beta7^+$ $Flt3^-$ $CD25^-$) and ILC2 precursor (ILC2P: $CD45^+$ Lin^- $CD127^+$ $\alpha4\beta7^+$ $Flt3^-$ $CD25^+$) from bone marrow of WT mice; in common precursor to ILC (ILCP: $CD45^+$ Lin^- $cKit^+$ $CD127^+$ $\alpha4\beta7^+$ PLZF-GFP^+) from bone marrow of $PLZF^{GFP\text{-}Cre+/-}$. Absolute copy numbers per 40000 copies of *Actb* are shown in a and d. ND, =not detected. (**c, e**). Flow cytometry showing expression of distal Runx3-YFP by indicated cells in *Runx3d*$^{+/YFP}$ mice. Shaded histograms indicate wild-type mice. (**f**) Flow cytometry of CHILPs showing PLZF and distal Runx3-YFP expression in *Runx3d*$^{+/YFP}$ mice. Data are representative of at least two experiments (mean and s.d. of triplicates in a and d).

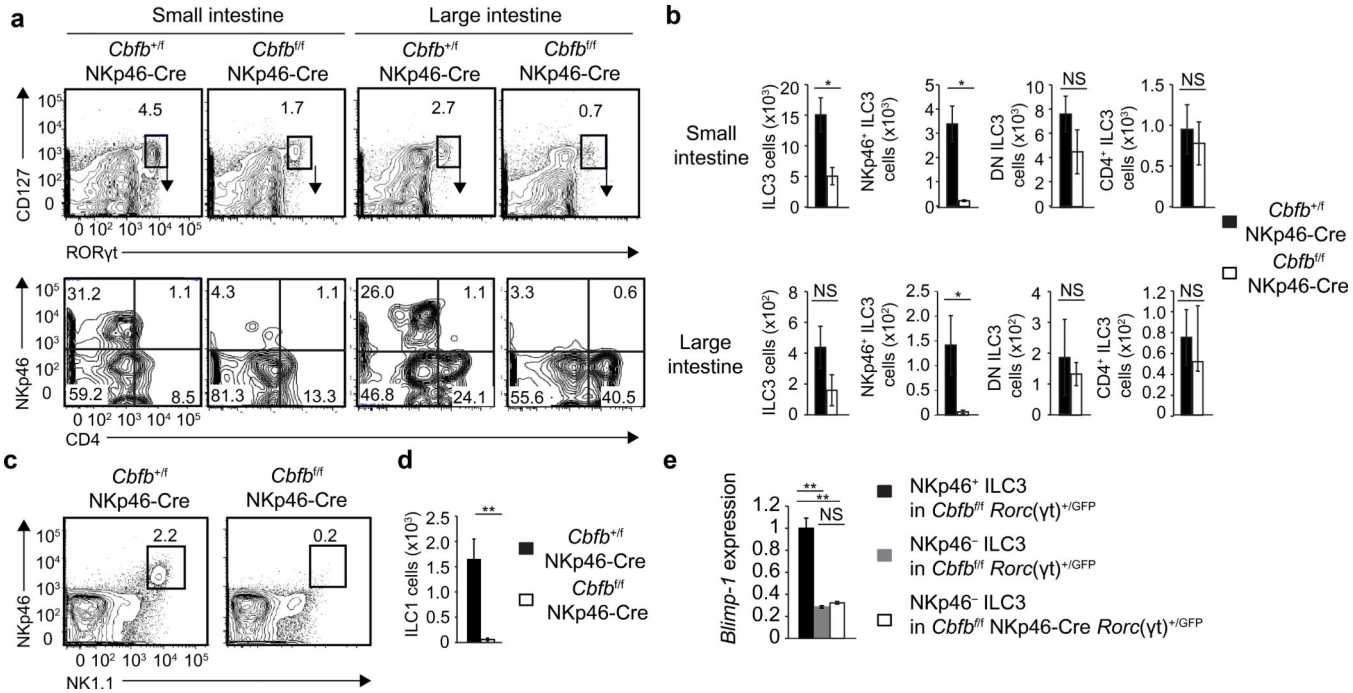

Figure 2.

Cbfb$^{f/f}$ NKp46-Cre mice lack NKp46^{+} ILC3 and ILC1 cells in intestine. (a) Flow cytometry of lamina propria lymphocytes (LPLs) showing ILC3 subsets in small and large intestine of *Cbfb*$^{+/f}$ NKp46-Cre and *Cbfb*$^{f/f}$ NKp46-Cre mice. Plots were gated on Live CD45^{+} CD3^{-} CD19^{-} cells. Numbers in outlined areas or quadrants indicate percent cells in each. Arrows in upper panels indicate gated cells shown in lower panels. (b) Absolute cell numbers of total ILC3 cells or indicated ILC3 subsets in LPLs from small intestine and large intestine of *Cbfb*$^{+/f}$ NKp46-Cre and *Cbfb*$^{f/f}$ NKp46-Cre mice. (c) Flow cytometry of intraepithelial lymphocytes (IELs) showing ILC1 cells in small intestine of *Cbfb*$^{+/f}$ NKp46-Cre and *Cbfb*$^{f/f}$ NKp46-Cre mice. Plots were gated on Live CD45^{+} CD3^{-} CD19^{-} cells. Numbers in outlined areas indicate percent cells in each. (d) Absolute cell numbers of ILC1 cells (CD45^{+} CD3^{-} CD19^{-} NK1.1^{+} NKp46^{+} CD49a^{+}) in IELs from small intestine of *Cbfb*$^{+/f}$ NKp46-Cre and *Cbfb*$^{f/f}$ NKp46-Cre mice. (e) Quantitative RT-PCR analysis showing *Blimp-1* expression in indicated ILC3 cells of small intestine from indicated mice, presented as relative to *Actb* expression (mean and s.d. of triplicates). Data are representative of more than three experiments (mean and s.d. of three mice in b and d). *$p < 0.05$ by Student's *t*-test. NS, not significant.

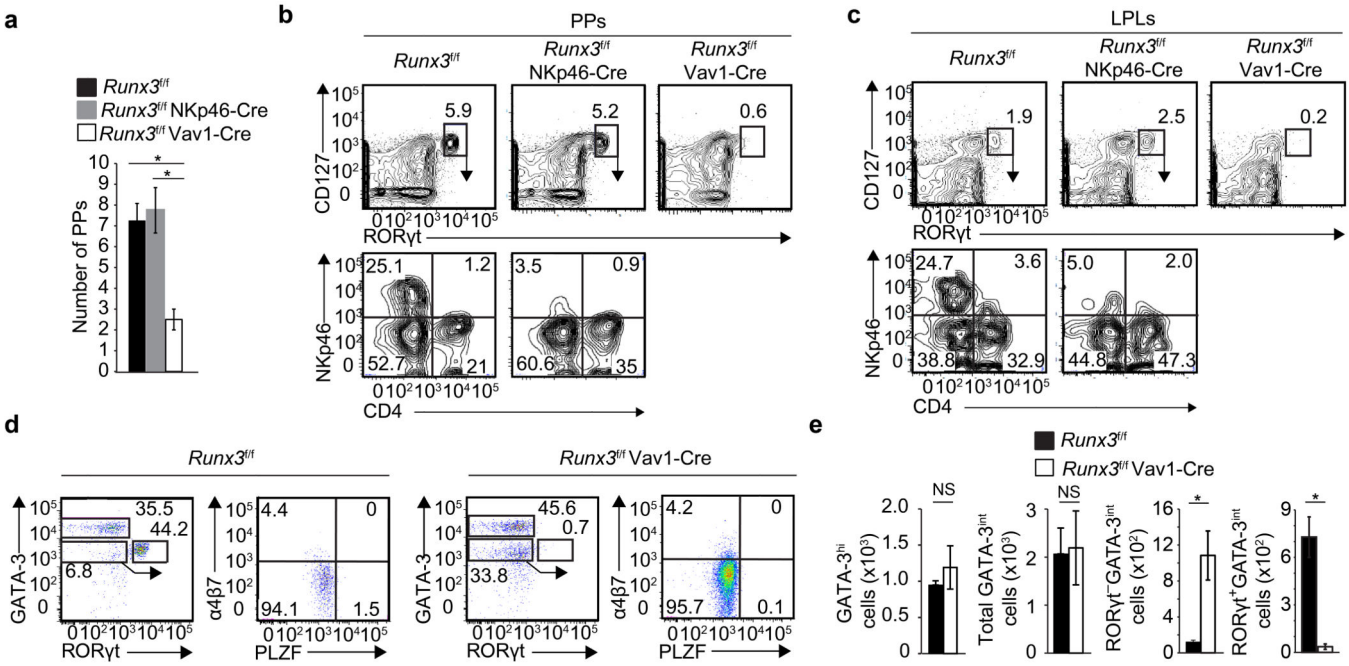

Figure 3.

Defects of ILC3 differentiation in *Runx3*$^{f/f}$ NKp46-Cre and *Runx3*$^{f/f}$ Vav1-Cre mice. (a) Number of Peyer's patches (PPs) in *Runx3*$^{f/f}$, *Runx3*$^{f/f}$ NKp46-Cre and *Runx3*$^{f/f}$ Vav1-Cre mice. (b, c) Flow cytometry of PP lymphocytes (b) or LPLs in large intestine (c) showing ILC3 subsets in *Runx3*$^{f/f}$, *Runx3*$^{f/f}$ NKp46-Cre and *Runx3*$^{f/f}$ Vav1-Cre mice. Plots were gated on Live CD45^{+} CD3^{-} CD19^{-} cells. Numbers in outlined areas indicate percent cells. Arrows in upper panels indicate gated cells shown in lower panels. (d) Flow cytometry of LPLs in large intestine of *Runx3*$^{f/f}$ and *Runx3*$^{f/f}$ vav1-Cre mice for GATA-3, RORγt, α4β7 and PLZF. Left plots were gated on Live CD45^{+} CD3^{-} CD19^{-} CD127^{+} NK1.1^{-} cells. Arrows in left panels indicate gated cells shown in right panels. (e) Absolute cell numbers of GATA-3^{hi} (ILC2) and GATA-3^{int} cells among CD45^{+} CD3^{-} CD19^{-} CD127^{+} NK1.1^{-} LPLs from large intestine of *Runx3*$^{f/f}$ and *Runx3*$^{f/f}$ vav1-Cre mice. Numbers in outlined areas or quadrants indicate percent cells in each. Data are representative of more than three independent experiments (mean and s.d of four mice in a, of three mice in e). $^{**}p < 0.01$ by Student's *t*-test. NS, not significant.

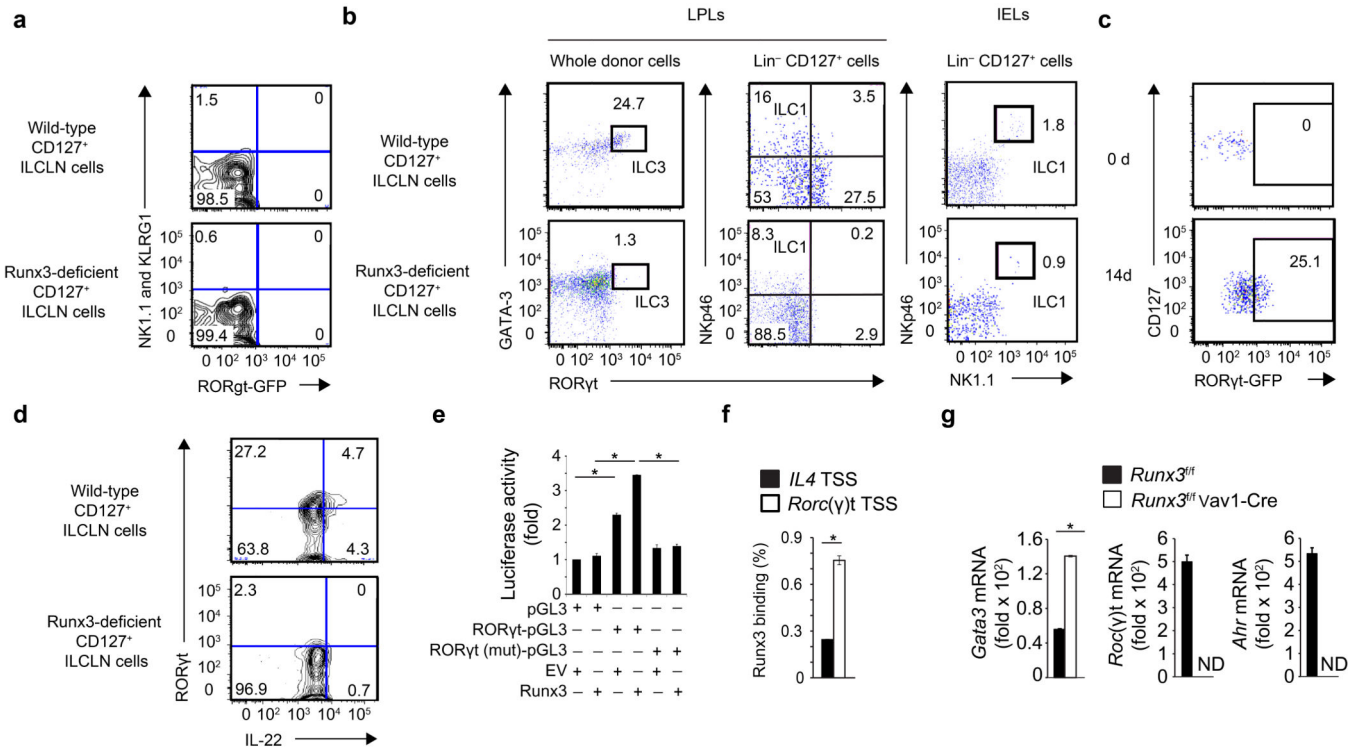

Figure 4.

Runx3 regulates RORγt and subsequent AHR expression in ILC3 cells. (a, b, c, d) Wild-type CD127^{+} ILCN cells from intestine of *Rorc*(γt)$^{+/GFP}$ mice and Runx3-deficient CD127^{+} ILCN cells from intestine of *Runx3*$^{f/f}$ Vav1-Cre mice were injected into *C. Rag2*$^{-/-}$ *Il2gc*$^{-/-}$ mice (a, b) or cultured *in vitro* (c, d). (a) Post sort analysis for indicated ILC markers. (b) Flow cytometry of donor H-2^{b+} cells in intestinal LPLs and IELs showing indicated ILC markers three months after injection. (c) Flow cytometry showing RORγt-GFP expression in wild-type CD127^{+} ILCN cells from *Rorc*(γt)$^{+/GFP}$ mice before culture and post 14 days culture. (d) Flow cytometry showing IL-22 production by cells derived from indicated input cells after 14 days in culture. (e) Luciferase activity in NK-92 cells transfected with pGL3, pGL3 with RORγt promoter (RORγt-pGL3), or pGL3 with mutations in Runx binding site of RORγt promoter (RORγt (mut)-pGL3) together with Runx3-expressing vector (Runx3) or empty vector (EV). (f) Chromatin immunoprecipitation assay showing Runx3 binding to *IL4* and *Roc*(γ)t transcription start sites (TSS) in ILC3 cells. (g) Quantitative RT-PCR analysis showing expression of indicated genes in CD45^{+} CD3^{-} CD19^{-} CD127^{+} NK1.1^{-} LPLs of the indicated mice, relative to *Actb* expression. Numbers in outlined areas or quadrants indicate percent cells in each. Data are representative of two independent experiments (a, b, c, d; mean and s.d. of triplicates in e, f, g). $^{**}p < 0.01$ by Student's *t*-test. ND, not detected.

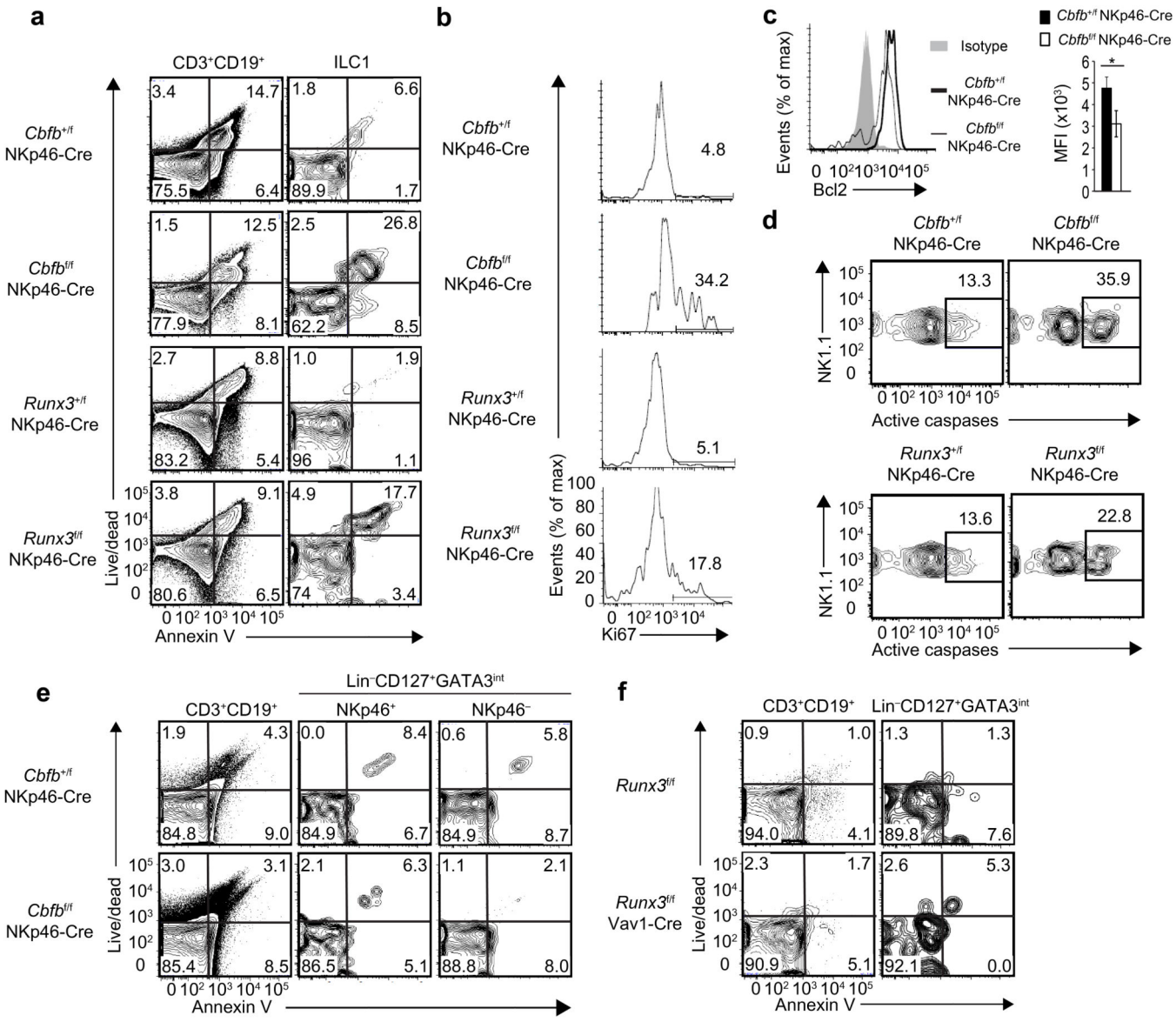

Figure 5.

Runx3 is essential for survival of ILC1 cells but not ILC3 cells. (a) Flow cytometry of $CD3^+$ $CD19^+$ cells, ILC1 cells ($CD45^+$ $CD3^-$ $CD19^-$ $NK1.1^+$ $NKp46^+$ $CD49a^+$) in intestine of *Cbfb*$^{+/f}$ NKp46-Cre, *Cbfb*$^{f/f}$ NKp46-Cre, *Runx3*$^{+/f}$ NKp46-Cre and *Runx3*$^{f/f}$ NKp46-Cre mice for apoptosis markers. (b, d) Flow cytometry showing expression of Ki-67 (b) and active caspases (d) in ILC1 cells of *Cbfb*$^{+/f}$ NKp46-Cre, *Cbfb*$^{f/f}$ NKp46-Cre, *Runx3*$^{+/f}$ NKp46-Cre and *Runx3*$^{f/f}$ NKp46-Cre mice. (c) Intestinal IELs of *Cbfb*$^{+/f}$ NKp46-Cre (thick line) and *Cbfb*$^{f/f}$ NKp46-Cre mice (thin line) were cultured with IL-15 (20ng/mL) for 24h and Bcl-2 expression by ILC1 cells were examined by flow cytometry (left, histograms; right, mean fluorescent intensity). Shaded histogram: isotype control. *$p < 0.05$ by Student's *t*-test. (e, f) Flow cytometry of $CD3^+$ $CD19^+$ cells, $CD45^+$ $CD3^-$ $CD19^-$ $CD127^+$ $NK1.1^-$ GATA-3^{int} Peyer's patch lymphocytes of *Cbfb*$^{+/f}$ NKp46-Cre and *Cbfb*$^{f/f}$ NKp46-Cre mice

(e) or *Runx3*$^{f/f}$ and *Runx3*$^{f/f}$ Vav1-Cre mice (f) for apoptosis markers. Data are representative of three independent experiments (mean and s.d. of three mice in c).

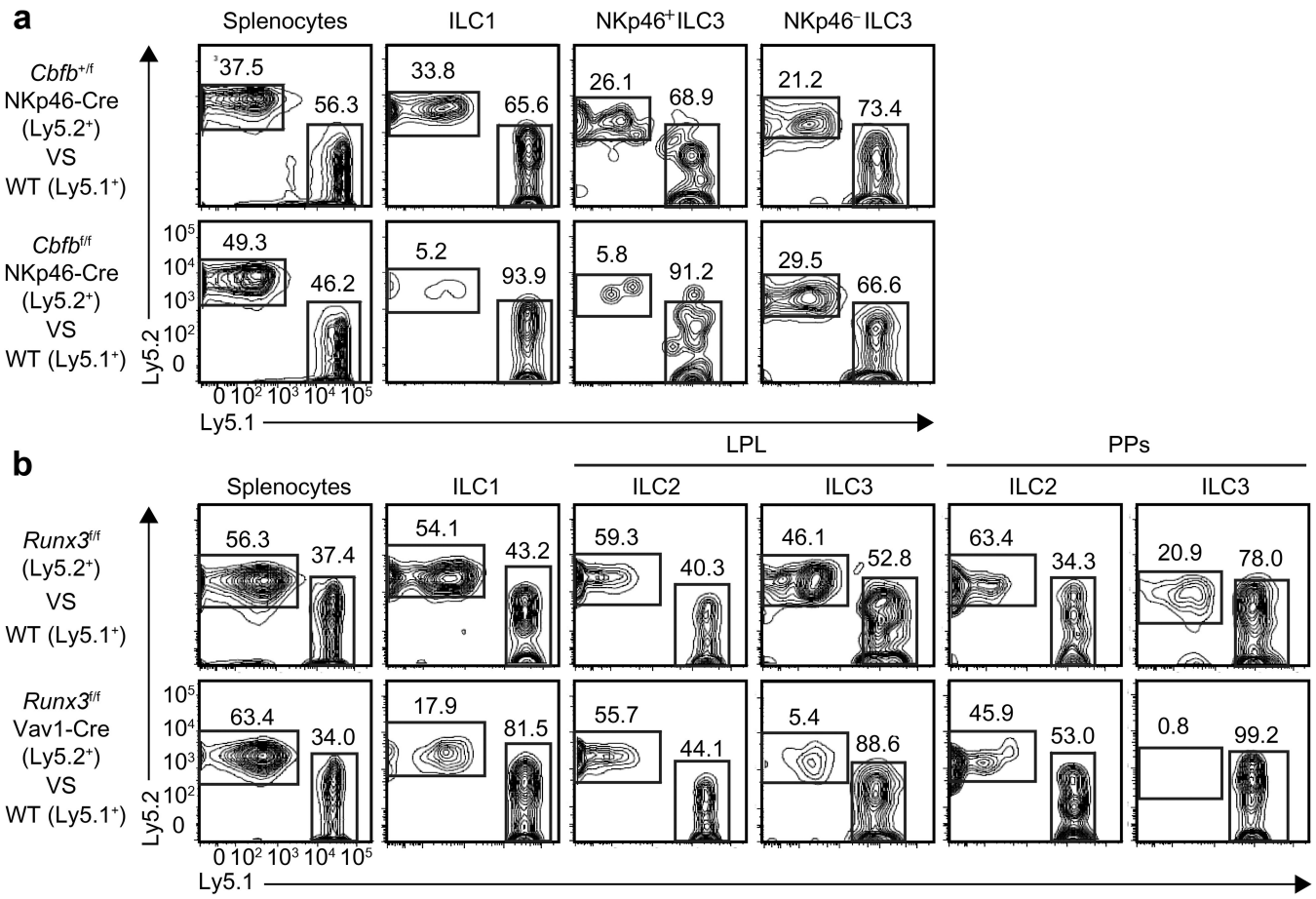

Figure 6.

Cell intrinsic requirement of Runx3 for development of ILC1 and ILC3 cells. (a, b) Fifty percent of Ly5.1 WT bone marrow cells and fifty percent of Ly5.2 bone marrow cells from *Cbfb*$^{+/f}$ NKp46-Cre, *Cbfb*$^{f/f}$ NKp46-Cre (a), *Runx3*$^{f/f}$ or *Runx3*$^{f/f}$ Vav1-Cre mice (b) were transferred into lethally irradiated Ly5.1 mice. Chimerism was determined by Ly5.1 and Ly5.2 expression of indicated cells in the chimeric mice by flow cytometry. ILC1 cells (CD45^{+} CD3^{-} CD19^{-} NK1.1^{+} NKp46^{+} CD49a^{+}) were from small intestine. ILC2 cells (CD45^{+} CD3^{-} CD19^{-} CD127^{+} GATA-3^{high}) and ILC3 cells (CD45^{+} CD3^{-} CD19^{-} CD127^{+} RORγt^{+}) were from small and large intestine (a, b) and PP lymphocytes (b). RORγt expression was detected by anti-RORγt staining. Numbers in outlined areas indicate percent cells in each. Data are representative of two independent experiments.

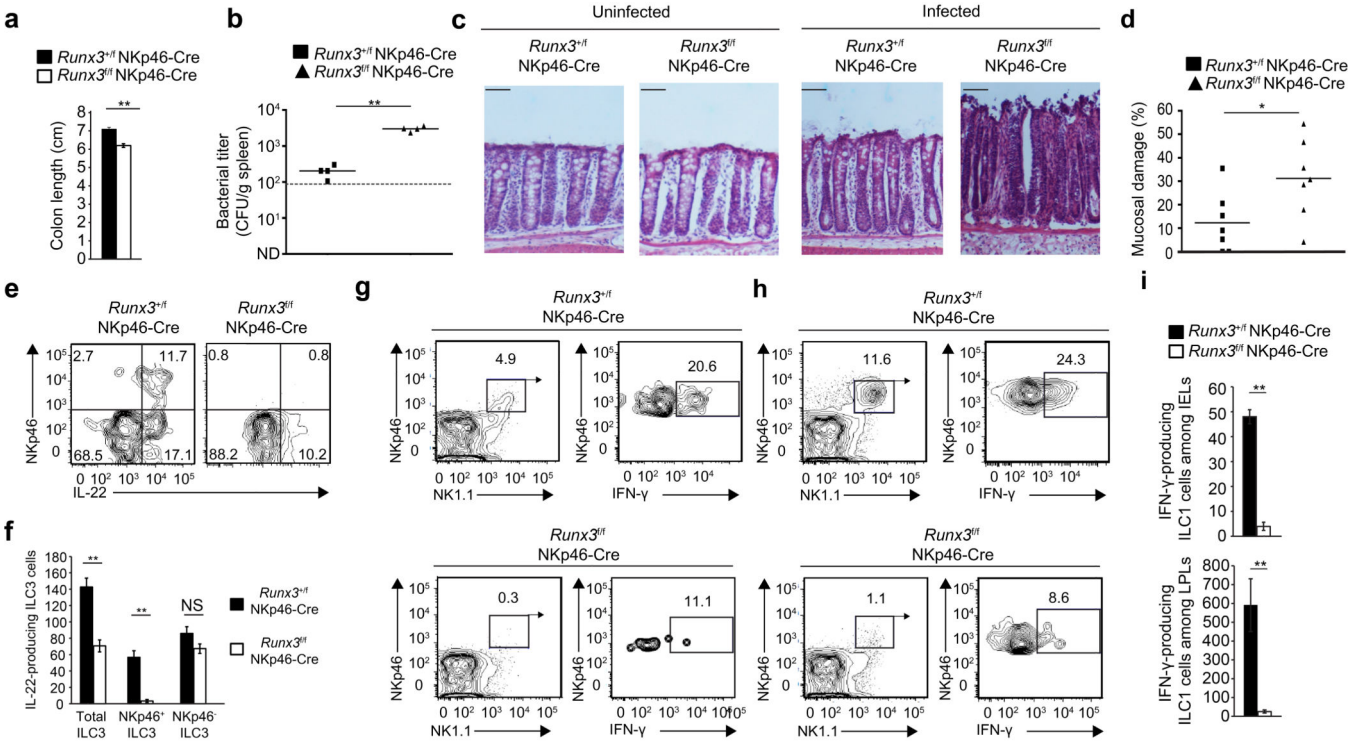

Figure 7.

Runx3 in ILC cells is critical to control acute infection with *C. rodentium*. (a-i) *Runx3*$^{+/f}$ NKp46-Cre and *Runx3*$^{f/f}$ NKp46-Cre mice were orally infected with *C. rodentium*. On day eight after infection, (a) length of colon, (b) titers of *C. rodentium* in spleen (dotted line, detection limit), (c) histology of colon (scale bars, 100 μm), (d) percentage of mucosal damage of colon, (e,f) IL-22 production by ILC3 cells in colon (e, frequency; f, absolute cell numbers) and (g–i) IFNγ production by ILC1 cells in colon (g, frequency in IELs; h, frequency in LPLs; i, absolute cell numbers) were examined. Numbers in outlined areas or quadrants indicate percent cells in each (e, g, h). Arrows in left panels in h indicate gated cells shown in right panels. Data are representative of more than three independent experiments (mean and s.d. of four mice in a and b, seven mice in d, three mice in f and i). *$p < 0.05$ and **$p < 0.01$ by Student's *t*-test. NS, not significant.